XRES from an [Er$_{22}$|Tb$_{22}$] Superlattice

J. Voigt,[1] D. Wermeille,[2] T. Brückel[1]

[1]Institute of Solid State Research, Research Centre Jülich, Jülich, Germany

[2]Ames Laboratory and Department of Physics and Astronomy, Iowa State University, Ames, IA, U.S.A.

Introduction

The magnetism of nanostructured materials fascinates scientists because of its relevance to understanding the influence of surfaces, interfaces, and electronic confinement. Applications of these materials in electronic devices open revolutionary windows because of the spin nature of their electrons.

Artificial superlattices containing rare-earth materials exhibit a variety of astonishing magnetic phenomena [1 and references therein]. Most noteworthy is the effect of interlayer exchange coupling (i.e., the formation of a coherent magnetic structure), even though nonmagnetic spacer layers separate the magnetic layers. Introducing spacer layers with a different magnetic structure leads to even more complex phases, as shown in Ref. 2.

The ground state of the pure elements is mainly determined by the subtle balance among the RKKY interaction, crystal field anisotropy, and magnetoelastic energy [3]. In a superlattice containing Er and Tb, the anisotropies are fairly different. Bulk Tb exhibits two ordered magnetic phases. For both ordered states, the magnetic moments are aligned within the basal plane of the hexagonal lattice due to the strong crystal field anisotropy. The helix phase is stable between 230 and 220K. Below 220K, the magnetic structure is simply ferromagnetic. Er, in contrast, shows a series of different ordered phases below 81K, with a preferred orientation along the c-direction. At temperatures below 20K, the c-axis component becomes ferromagnetic, while the basal plane component remains in a modulated structure.

The pure materials show strong magnetostriction when they become ferromagnetic, exemplifying the influence of the magnetoelastic energy. It is evident that the epitaxial strains in a superlattice affect the magnetic structure. In a superlattice containing Er and Tb, magnetic proximity effects and the competing anisotropies affect the magnetic ground state. In our work, we are investigating the magnetic structure of a series of [Er|Tb] superlattices with different compositions in order to systematically study the influence of the different contributions.

Methods and Materials

The superlattice was grown by molecular beam epitaxy (MBE) on a sapphire substrate. The recipe given in Ref. 1 was followed to evaporate a buffer containing 250 Å of Nb and 600 Å of Y onto the substrate, providing a smooth (0001) surface of Y. The growth conditions were optimized by *in situ* low-energy electron diffraction (LEED) and Auger electron spectroscopy. At a substrate temperature of 350K, the surface mobility was good enough to yield single crystalline surfaces and to suppress interdiffusion. The superlattice contains 80 bilayers, each composed of 22 atomic layers of Er and 22 atomic layers of Tb.

Neutron diffraction revealed the magnetic structure of the superlattice. Below 230K, magnetic moments align ferromagnetically within single bilayers. Neighbored bilayers are coupled antiferromagnetically. The phase transition temperature is roughly identical to the Néel temperature of metallic Tb, when the helix sets in. Below 100K, a magnetic modulation is found. The correlation length deduced from the width of the magnetic reflection is about 60 Å, equal to the thickness of a single Er layer. The phase transition temperature cannot be precisely determined because of the bad signal-to-noise ratio.

To study the magnetic behavior of the film specific elements, we measured the x-ray resonant exchange scattering (XRES) from the specimen. When the energy of the incoming photons was tuned to the absorption edge of the elements, the resonant enhancement of the magnetic scattering provided information about the magnetic state of the respective material only. The sample was mounted to a closed-cycle cryostat. The sample temperature could be varied between 6 and 300K at an accuracy of better than 1K. A vertical scattering geometry was chosen. In order to suppress the dominant charge scattering, the polarization of the scattered photons was analyzed. We chose a vertical scattering geometry to analyze the polarization in σ-π' geometry (i.e., we measured the component of the scattered light that was rotated by the resonant magnetic scattering process). In contrast, charge scattering left the polarization state unchanged. The charge scattering was suppressed by 95% at the Er L$_{III}$ edge and by more than 99% at the Tb L$_{III}$ edge. The high efficiency at the Tb edge could be achieved by using an Al(222) crystal. At the Er edge, we employed a pyrolitic graphite crystal using the (0006) reflection.

Results

Longitudinal scans in reciprocal space along the (000Q_z) direction for photon energies close to the Er
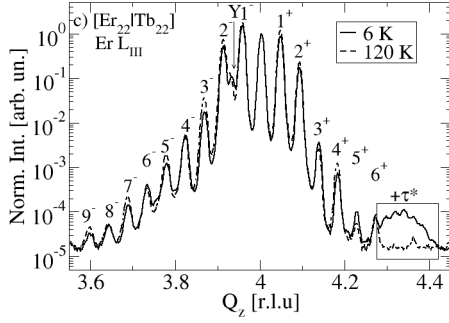
FIG. 1. Scans [000Q_z] at different temperatures close to the Er L_{III} edge (E = 8.359 keV). The broad feature 4.27 < Q_z < 4.37 is related to a short-range-ordered magnetic modulation.

L_{III} edge are shown in Fig. 1 for different temperatures. The superlattice periodicity is illustrated by the satellite reflections due to the squared chemical structure. The superlattice peaks are resolved up to the order of 10, confirming the good sample quality.

The short-range-ordered magnetic modulation leads to the broad feature shown at the high-Q_z side of the spectrum. The reflection is very well separated from the background. The broad diffuse XRES is due to virtual excitation of core electrons into the 5d conduction band of Er, with subsequent decay and reemission of a photon. The density of unoccupied states is exchange-split in magnetically ordered material; hence, XRES probes the polarization in the respective band. The polarization is coherent only within a single Er layer. The XRES results prove that the magnetic modulation is restricted to single Er layers. Furthermore, the strong signal allows a more precise determination of the phase transition temperature and the temperature dependence
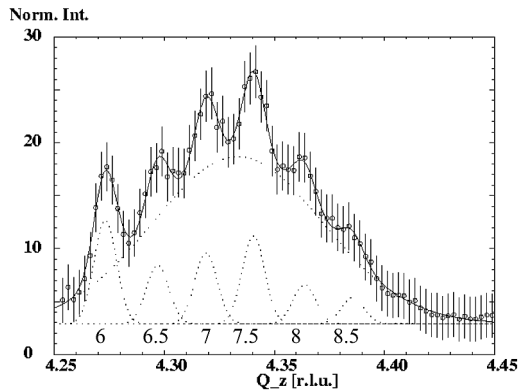
FIG. 2. Longitudinal scan [000Q_z] at 10K (E = 8.361 keV). Integer indices refer to the chemical superstructure and half integer to a superlattice with a doubled super cell (i.e., antiferromagnetic coupling of ferromagnetically ordered layers).t-range-ordered magnetic modulation.

of the modulation vector. The diffuse scattering cannot be detected above 80K; therefore, the phase transition in both the superlattice and the bulk Er sample take place at almost exactly the same temperature.

One also notices small peaks on top of the broad diffuse scattering. They become clearer on the linear scale in Fig. 2. They are related to the superstructure of the sample. The reflections indexed with integer numbers originate from the chemical superstructure. Half integer indices point to a doubling of the super cell, as caused by the antiferromagnetic coupling of ferromagnetically ordered layers. The energy dependence of the half-integer reflections proves the magnetic origin (Fig. 3).

The diffuse scattering and the half-integer superlattice peak reveal double-peak resonance behavior, while the energy dependence of the integer superlattice peak is typical for a charge scattering reflection.

The half-integer reflections vanish at the same temperatures as does the diffuse scattering. In contrast,
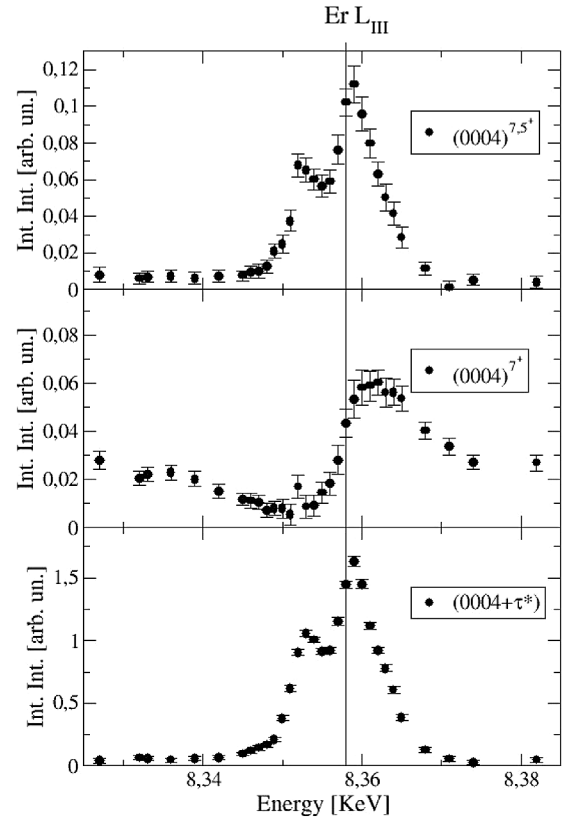
FIG. 3. Integrated intensity of the diffuse scattering (0004 + τ^*), the integer superlattice peak (0004)[7+], and the half-integer superlattice peak (0004)[7.5+] as a function of energy at T = 10K. The inflection point of the fluorescence (not shown) determines the position of the absorption edge.
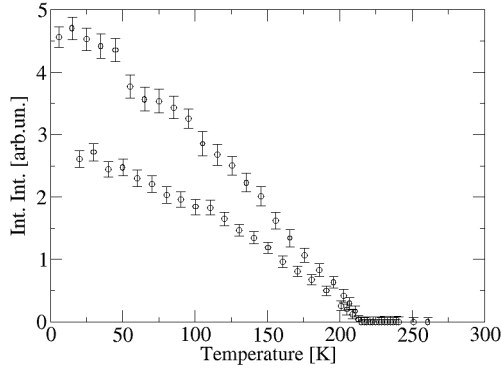
FIG. 4. Integrated intensity of the half-integer superlattice peak $(0004)^{0.5-}$ as a function of temperature. The photon energy $E = 7.518$ is close to the Tb L_{III} absorption edge.

we observe half-integer peaks close to the Tb L_{III} absorption edge above the "background" of charge scattering from the superlattice up to a temperature of 215K (Fig. 4). Polarization due the ferromagnetic order exists in the Tb conduction band for all temperatures when the 4f moments are ordered, while polarization can be observed in the Er only when the short-range-ordered modulated phase is present. Because of the less efficient polarization analysis, we cannot determine whether half-integer reflections with a lower index exist at the Er absorption edge.

We emphasize the fact that the antiferromagnetic coupling tends to be unstable. The temperature dependence in Fig. 4 was measured starting from 20K after the sample remained at low temperatures for more than 2 days. Heating to the paramagnetic state and subsequent cooling to 6K resulted in higher intensity for the half-integer reflections. The same behavior was observed by neutron diffraction.

Discussion

The sample exhibits an antiferromagnetic coupling of ferromagnetic Tb layers below 230K. At the Tb edge, we observe the respective polarization in the Tb conduction band below roughly 215K. However, it is difficult to make any observations close to the phase transition because of the dominant charge reflection.

The Er layers form a magnetic modulation at temperatures similar to those found in bulk material. In conjunction with the spin density wave of the short-range magnetic modulation, higher-order components of the antiferromagnetic coupling appear in the 5d conduction band of Er.

These results confirm the assumption that the antiferromagnetic coupling at high temperatures is driven by dipolar magnetic interactions between ordered Tb layers. At low temperatures, the magnetic ordering within the Er layers introduces a competing interaction that weakens the coupling. Neutron diffraction reveals increasing diffuse scattering with decreasing temperature, which could be explained by the formation of small, ferromagnetically coupled domains.

Polarized neutron scattering at grazing incidence probes the domain structure of the sample. The first measurements have shown that ferromagnetic coupling is established if the sample is cooled in a modest magnetic field. Results of our complementary work using x-ray and neutron scattering will be published elsewhere.

Acknowledgments

References

[1] C.F. Majkrzak et al., Adv. Phys. **40**, 99 (1991).
[2] R.A. Cowley, J. Magn. Magn. Mater. 177-181, 1156 (1998).
[3] J. Jensen and A.R. Macintosh, *Rare Earth Magnetism* (Oxford University Press, 1991).